

Probing Universal Extra Dimension at the International Linear Collider

Gautam Bhattacharyya¹, Paramita Dey¹, Anirban Kundu², and Amitava Raychaudhuri²

¹⁾ *Saha Institute of Nuclear Physics, 1/AF Bidhan Nagar, Kolkata 700064, India*

²⁾ *Department of Physics, University of Calcutta, 92 A.P.C. Road, Kolkata 700009, India*

Abstract

In the context of an universal extra-dimensional scenario, we consider production of the first Kaluza-Klein electron positron pair in an e^+e^- collider as a case-study for the future International Linear Collider. The Kaluza-Klein electron decays into a nearly degenerate Kaluza-Klein photon and a standard electron, the former carrying away missing energy. The Kaluza-Klein electron and photon states are heavy with their masses around the inverse radius of compactification, and their splitting is controlled by radiative corrections originating from bulk and brane-localised interactions. We look for the signal event $e^+e^- +$ large missing energy for $\sqrt{s} = 1$ TeV and observe that with a few hundred fb^{-1} luminosity the signal will be readily detectable over the standard model background. We comment on how this signal may be distinguished from similar events from other new physics.

PACS Nos: 12.60.-i, 14.60.Hi

Key Words: Universal Extra Dimension, International Linear Collider

Introduction: If extra-dimensional models in a few hundred GeV scale [1] are realised in Nature, one can not only undertake their precision studies at the proposed International Linear Collider (ILC) [2] but also can distinguish them from other new physics. In this paper, we consider such models with one extra dimension having inverse radius of compactification in the range $R^{-1} = 250 - 450$ GeV. We examine production of the first Kaluza-Klein (KK) electron positron pair ($E_1^+ E_1^-$) in a linear e^+e^- collider operating at $\sqrt{s} = 1$ TeV. The heavy modes E_1^\pm would decay into the standard (zero modes) e^\pm and the first KK photon (γ_1), the latter carrying away missing energy. The splitting between E_1^\pm and γ_1 comes from the bulk and brane-localised radiative corrections. The cross section of the final state e^+e^- plus missing energy is quite large and the standard model (SM) background is tractable, so that even with a one year run of ILC at $\sqrt{s} = 1$ TeV with approximately 300 fb^{-1} enough statistics would accumulate. Forward-backward asymmetry of the final state electron mildly depends on the initial polarisations. Even though the mass spectrum of KK excitations of different SM particles may resemble the supersymmetric pattern, angular distribution of the final electrons can be used to discriminate the intermediate KK electrons from selectrons or other new physics scalars.

Simplest universal extra dimension: We consider the simplest realisation of the universal extra dimension (UED) scenario in which there is only one extra dimension which is accessed by all SM particles [3]. The extra dimension (y) is compactified on a circle of radius R along with a Z_2 orbifolding which renders all matter and gauge fields, viewed from a 4 dimensional (4d) perspective, depend on y either as $\cos(ny/R)$ (even states) or $\sin(ny/R)$ (odd states), where n is the KK index. The tree level mass of the n th state of a particular field is given by $M_n^2 = M_0^2 + n^2/R^2$, where M_0 is the zero mode mass of that field. Clearly, excepting the top quark, Higgs, W , and Z , the KK states of all other SM particles with the same n are nearly mass degenerate at n/R . Now, with all the fields propagating in the bulk, the momentum along the fifth direction, quantised as n/R , remains a conserved quantity. A closer scrutiny however reveals that a remnant Z_2 symmetry (different from the previous Z_2) in the effective 4d Lagrangian dictates that what actually remains conserved is the KK parity

R^{-1}	ΛR	$M_{\hat{\mathcal{E}}_1}$	$M_{\mathcal{E}_1}$	M_{W_1}	M_{Z_1}	M_{γ_1}
250	20	252.7	257.5	276.5	278.1	251.6
	50	253.6	259.7	280.6	281.9	251.9
350	20	353.8	360.4	379.0	379.7	351.4
	50	355.0	363.6	384.9	385.4	351.5
450	20	454.9	463.4	482.9	483.3	451.1
	50	456.4	467.5	490.6	490.8	451.1

Table 1: KK masses ($n = 1$) for different cases: excited electrons in SU(2) singlet and doublet representations, excited charged and neutral gauge bosons, respectively. All mass scales are in GeV.

defined as $(-1)^n$. As a result, level mixings may occur which admit even states mix only with even states, and odd with odd. Therefore, (i) the lightest Kaluza-Klein particle (LKP) is stable, and (ii) a single KK state (e.g. $n = 1$ state) cannot be produced. These two criteria are reminiscent of supersymmetry with conserved R-parity where the lightest supersymmetric particle (LSP) is stable, and superparticles can only be pair produced. If produced, the heavier KK modes can cascade decay to lighter ones, eventually to soft SM particles plus LKP carrying away missing energy. But low energy constraints on the UED scenario from $g - 2$ of the muon [4], flavour changing neutral currents [5, 6, 7], $Z \rightarrow b\bar{b}$ decay [8], the ρ parameter [3], other electroweak precision tests [9] and implications from hadron collider studies [10], all indicate that $R^{-1} \gtrsim$ a few hundred GeV. As a result, even the second KK state having mass $2/R$ will be beyond the pair-production reach of at least the first phase of the planned linear collider. So, as mentioned in the Introduction, we consider the production of first KK electron positron pair and their subsequent decays into first KK photon plus the standard leptons; the degeneracy between E_1^\pm and γ_1 being lifted by radiative corrections which we shall briefly touch upon below.

Radiative corrections and the spectrum: Barring zero mode masses, the degeneracy (n/R) at a given KK level is only a tree level result. Radiative corrections lift this degeneracy [11, 12, 13, 14]. For intuitive understanding, we consider the kinetic term of a scalar field as [11] $L_{\text{kin}} = Z\partial_\mu\phi\partial^\mu\phi - Z_5\partial_5\phi\partial^5\phi$ ($\mu = 0, 1, 2, 3$), where Z and Z_5 are renormalisation constants. Recall, tree level KK masses ($M_n = n/R$) originate from the kinetic term in the y -direction. If $Z = Z_5$, there is no correction to those KK masses. But this equality is a consequence of Lorentz invariance. When a direction is compactified, Lorentz invariance is lost, so also is lost the equality between Z and Z_5 , leading to $\Delta M_n \propto (Z - Z_5)$. One actually encounters two kinds of radiative corrections.

(a) *Bulk corrections:* These corrections are finite. Moreover, they are nonzero only for bosons. They arise when the internal loop lines wind around the compactified direction, sensing that compactification has actually occurred, leading to the breaking of Lorentz invariance. The correction to the KK mass M_n works out to be independent of n and goes like $\Delta M_n^2 \propto \beta/16\pi^4 R^2$, where β is a symbolic representation of the collective beta function contributions of the gauge and matter KK fields floating inside the loop. Since the beta function contributions are different for particles in different representation, the KK degeneracy is lifted. One can understand the decoupling of the correction as inverse power of R by noting that the $R \rightarrow \infty$ limit makes the fifth direction uncompactified leading to exact Lorentz invariance. For the KK fermions this correction is zero.

(b) *Orbifold corrections:* Orbifolding additionally breaks translational invariance in the fifth direction. The corrections to the KK masses arising from interactions localized at the fixed points are not finite unlike the bulk corrections. These are logarithmically divergent. These boundary terms can be thought of as counterterms whose finite parts are completely undetermined. A rather bold but predictive hypothesis is to assume that these corrections vanish at the cutoff scale Λ . Calculation shows that the correction to M_n does depend on M_n in this case, and a generic correction looks like $\Delta M_n \sim M_n(\beta/16\pi^2) \ln(\Lambda^2/\mu^2)$, where μ is the low energy scale where we compute these corrections. The KK states are thus further split, this time with an additional dependence on Λ .

Spectrum: The mass spectra of the first excited electrons and the first excited W^\pm, Z and photon for different choices of R and Λ are displayed in Table 1. While the tree level KK mass is given by $1/R$, the radiative corrections to them depend both on R and Λ (for the exact expressions, see, e.g.,[11]).

Production and decay modes of KK leptons: The SU(2) doublet KK states appear with both left and right chiralities as $\mathcal{L}_{L,R}$, where $\mathcal{L} = (\mathcal{N}_n, \mathcal{E}_n)^T$, so do the SU(2) singlets $\hat{\mathcal{E}}_{L,R}$. All these states for $n = 1$ will be pair produced at the foreseeable collider energy. As noted in Table 1, the orbifold corrections create enough mass splitting between these states and γ_1 (dominantly B_1) allowing the former to decay within the detector to $e^\pm +$ missing energy which constitute our signal. Below we denote \mathcal{E}_1^\pm and $\hat{\mathcal{E}}_1^\pm$ collectively by E_1^\pm .

Now we consider the pair production $e^+e^- \rightarrow E_1^+E_1^-$ for different polarisations of the incident beams. The interaction proceeds through s - and t -channel graphs. The s -channel processes are mediated by γ and Z . The t -channel processes proceed through γ_1/Z_1 gauge bosons and γ_1^5/Z_1^5 scalars (fifth components of 5d neutral gauge bosons). E_1 decays into e and γ_1 . The splitting between E_1 and γ_1 masses is sufficient for the decay to occur well within the detector with a 100% branching ratio (BR). It may be possible to observe even a displaced vertex (e.g., $\hat{\mathcal{E}}_1$ decays, for $R^{-1} = 250$ GeV). So in the final state we have $e^+e^- + 2\gamma_1$ (\equiv missing energy).

The same final state can be obtained from $e^+e^- \rightarrow W_1^+W_1^-$ as well. Again, the interaction proceeds through γ and Z mediated s -channel graphs, and \mathcal{N}_{1L} mediated t -channel graphs. Given the splittings (Table 1), W_1^\pm can decay into e_i^\pm and \mathcal{N}_{1i} , as well as into E_{1i}^\pm and ν_i , where $i = 1$ to 3 is the flavour index. While \mathcal{N}_{1i} escapes undetected, E_{1i}^\pm decays into e_i^\pm and γ_1 . So, if we tag only electron flavours (plus missing energy) in the final state, the $e^+e^- \rightarrow W_1^+W_1^-$ cross section, which is in the same ball-park as the $e^+e^- \rightarrow E_1^+E_1^-$ cross section, should be multiplied by a BR of $\sim 1/9$. Numerically, therefore, this channel is not significant. Even more insignificant contribution would come from $(W_1^5)^\pm$ scalar (fifth component of 5d charged gauge bosons) pair production.

SM background: The main background comes from $\gamma^*\gamma^* \rightarrow e^+e^-$ events, where γ^* s originate from the initial electron-positron pair while the latter go undetected down the beam pipe [15]. The $\gamma^*\gamma^*$ production cross section is $\sim 10^4$ pb. About half of these events results in final state e^+e^- pair as visible particles.

The background e^+e^- pairs are usually quite soft and coplanar with the beam axis [16]. An acoplanarity cut significantly removes this background. Such a cut, we have checked, does not appreciably reduce our signal. For example, excluding events which deviate from coplanarity within 40 mrad reduces only 7% of the signal cross section. In fact, current designs of LC envisage very forward detectors to specifically capture the ‘would-be-lost’ e^+e^- pairs down the beam pipe¹.

Numerically less significant backgrounds would come from $e^+e^- \rightarrow W^+W^-$, $e\nu W$, e^+e^-Z , followed by the appropriate leptonic decays of the W and Z .

Collider parameters: The study is performed in the context of the ILC [2], running at $\sqrt{s} = 1$ TeV (upgraded option), and with a polarisation efficiency of 80% for e^- and 50% for e^+ beams. We impose kinematic cuts on the lower and upper energies of the final state charged leptons as 0.5 and 20 GeV respectively. While the lower cut is a requirement for minimum energy resolution for identification, the (upper) hardness cut eliminates most of the SM background. We also employ a rapidity cut admitting only those final state electrons which are away from beam pipe by more than 15° .

Cross sections: The cross section for e^+e^- plus missing energy final state has been plotted in Fig. 1. We have neglected the events coming from excited W decay. Notice that varying the beam polarisations does create a detectable difference in the cross section, nevertheless, there is no special gain for any particular choice: for left-polarised e^- beam, both B_1 and W_1^3 contribute, whereas for the right-polarised e^- beam, only B_1 contributes but with an enhanced coupling. The cross section enhances as we increase ΛR from 2 to 20; this is due to the change in θ_{W_1} (the weak angle for $n = 1$ KK gauge bosons). Further increase of ΛR does not change the cross

¹To counter the two-photon background we may also advocate the following strategy. Instead of eliminating the background, we calculate the number of e^+e^- events originating from two-photon production. For this we first count the number of $\mu^+\mu^-$ plus missing energy events. The number of such events coming from the decay of KK muons, we have checked for $1/R \sim 250 - 300$ GeV, would be rather small, about a factor of 1/20 compared to the number of e^+e^- plus missing energy events, due to strong s -channel suppression. So most of the observed $\mu^+\mu^-$ events would have sprung from $\gamma^*\gamma^*$. Thus the muon events serve as a normalisation to count the e^+e^- plus missing energy events originating from the two-photon background. Our signal events should be recognized as those which are in excess of that. Based on the estimates of two-photon events given by the Colorado group [15], we have checked that for an integrated luminosity of 300 fb^{-1} the signal events would be about ten times larger than the square-root of background.

section; a saturation point is reached. Additionally, the kinematic cuts tend to reduce the cross section which is why the curve for $\Lambda R = 50$ lies between the ones for $\Lambda R = 2$ and 20.

Forward-backward (FB) asymmetries: The FB asymmetries of the final state electrons, defined as $A_{\text{FB}} = (\sigma_{\text{F}} - \sigma_{\text{B}})/(\sigma_{\text{F}} + \sigma_{\text{B}})$, are plotted in Fig. 2 for different values of ΛR . The reason as to why it falls with increasing $1/R$ is as follows. The first-stage process $e^+e^- \rightarrow E_1^+E_1^-$ is forward-peaked, and for smaller $1/R$, i.e. lighter KK electrons, the final state e^\pm are boosted more along the direction of the parent E^\pm . As $1/R$, or equivalently the KK mass, increases the boost drops and the distribution tends to lose its original forward-peaked nature. Polarisation of the beams does not appear to have a marked advantage. A point to note is that the electrons coming from two-photon background will be FB symmetric.

Discriminating UED from other new physics: It is not our purpose in this brief note to discuss at depth any specific version of new physics model and its possible discrimination from UED. Still, for illustrative purposes, we recall that the spectrum of KK excitations for a given level (here $n = 1$) may be reminiscent of a possible supersymmetry spectrum [17], where the KK parity is ‘like’ the R-parity. Even in a situation when the LSP weighs above 250 GeV and conspires to be almost degenerate with the selectron, it is possible to discriminate a KK electron decaying into the KK photon (LKP) from a selectron decaying into a neutralino LSP by studying the angular distribution pattern of the final state electron. We demonstrate this with a simple toy example. Compare the pair production of (a) generic heavy fermions and (b) generic heavy scalars in an e^+e^- collider in a toy scenario. Assume $\sqrt{s} \gg m$, where m is the mass of the heavy lepton/scalar, so that only the t -channel diagrams, with just a heavy gauge boson in case (a) and a heavy fermion in case (b) as propagators, are numerically dominant (we assume this only for the ease of analytic comparison). The heavy states are produced with sufficient boost, therefore the tagged leptons they decay into have roughly the same angular distributions as them. Take the mass of the t -channel propagator in either case to be about the same as the mass of the heavy lepton/scalar as $m = 250$ GeV. For these choices, the ratio of $d\sigma/d\cos\theta$ (case (a)/ case (b)) is observed to be $(3.8 + 1.3 \cos\theta + 0.6 \cos^2\theta)/\sin^2\theta$, clearly indicating that the two cases can be easily distinguished from their angular distributions. Moreover, the UED cross section is found to be a factor of 4 to 5 larger than the scalar production cross section for similar couplings and other parameters. For selectron production, indeed one must take the detailed neutralino structure and the exact couplings, but the basic arguments that we advanced for distinguishing scalar- from the fermion-productions at the primary vertex using the toy model would still hold.

Comparison with the CLIC Working Group study: Our analysis is complementary to that in the CLIC multi-TeV linear collider study report [18]. While we have electrons in the final state, the study in [18] involves muons. Clearly, the angular distribution in our case is dominated by t -channel diagrams, while the process studied in [18] proceeds only through s -channel graphs. Due to the inherently forward-peaked nature of the t -channel diagrams, we obtain a significantly larger FB asymmetry. Unlike in [18], we have neither included the initial state radiation effect nor incorporated detector simulation.

LHC/ILC synergy: Extensive studies have been carried out [19] addressing the physics interplay between the LHC and the ILC, in particular, how the results obtained at one machine would influence the way analyses would be carried out at the other. While LHC may serve as a discovery machine, precision measurements of the masses, decay widths, mixing angles, etc., of the discovered particles can be carried out at the ILC. To illustrate this with an example, let us consider a selectron weighing around 200 GeV. The analysis [20] shows that while the uncertainty in its mass determination is around 5 GeV at the LHC, with inputs from the ILC the uncertainty can be brought down to about 0.2 GeV due to a significantly better edge analysis in the clean ILC environment. Similar precisions may be expected for the masses of the KK electrons as well for a comparable cross-section. However, if R^{-1} is large and the cross section goes down by about a factor of 50-100, the sensitivity will also go down scaling inversely as the square root of the number of events. (Beam polarisation will not be of much help, as can be seen from Fig. 1). Another point that may play a significant role in determining the masses is the softness of final-state electrons. We have applied adequate softness cuts to remove very soft electrons. One needs a detailed analysis to determine the exact accuracies at different benchmark points, but roughly the accuracy of determining the KK masses at the ILC should be of the order of 1 GeV or even better. Even if the KK electrons are first observed at the LHC, their spin assignments might not be possible. This particular issue, i.e. whether UED states can be distinguished from the supersymmetric

states at the LHC, has been studied in [21]. Considering the decay chain in which a KK quark (or, a squark) disintegrates into a quark, a lepton-antilepton pair and missing energy, and looking at the spin correlations of the emitted quark with one of the leptons, the authors of [21] conclude that for a quasi-degenerate (UED like) spectrum, spin assignments of the discovered particles could hardly be efficiently done: the best discriminator of UED from supersymmetry in that case would be a significantly larger production cross sections for the UED particles than those of the supersymmetric ones. On the contrary, if the observed spectrum is hierarchical (e.g. a supersymmetric type), the prospects of observing spin correlations would be better. However, the ILC would provide a better environment for doing spin studies. The clinching evidence of UED would of course be the discovery of the $n = 2$ KK modes. While the Z_2 peak can be discovered at the LHC through some hadronically quiet channels, γ_2 will be hard to detect at the LHC because it immediately decays into two jets which will be swamped by the QCD background [22]. Turning our attention now to the ILC, given its proposed energy reach, these states will too heavy to be pair produced, but as shown in [22], single resonant productions of Z_2 and γ_2 , despite suppression from KK number violating couplings, will have sizable cross sections. Precision measurements of their peak positions and widths at the ILC will enable one to extract R and Λ .

Conclusion: We have shown that the ILC may have a significant role in not only detecting the presence of few-hundred-GeV-size extra dimensions but also discriminating it from other new physics options, like supersymmetry. Even if the KK modes are first observed at the LHC, one needs the ILC for their proper identification through precision measurements of the masses, couplings and spin correlations. The physics interplay of the LHC and the ILC will be quite important in this context.

Acknowledgements

We thank H.C. Cheng for clarifying to us some aspects of orbifold radiative corrections. We acknowledge very fruitful correspondences with M.E. Peskin on the two-photon background. We also thank J. Kalinowski for presenting a preliminary version of this work in ICHEP 2004, Beijing [23]. Thanks are also due to S. Dutta and J.P. Saha, who were involved in the earlier stages of this work. Stimulating discussions with the participants of the Study Group on Extra Dimensions at LHC, held at HRI, Allahabad, are also acknowledged. G.B., P.D., and A.R. acknowledge hospitality at Abdus Salam ICTP, Trieste, while G.B. also acknowledges hospitality at LPT, Orsay, and Theory Division, CERN, at different stages of the work. G.B. and A.R. were supported, in part, by the DST, India, project number SP/S2/K-10/2001. AK was supported by DST, Govt. of India, through the project SR/S2/HEP-15/2003.

References

- [1] I. Antoniadis, Phys. Lett. B **246** (1990) 377.
- [2] D. J. Miller, arXiv:hep-ph/0410306.
- [3] T. Appelquist, H.C. Cheng and B.A. Dobrescu, Phys. Rev. D **64** (2001) 035002 [arXiv:hep-ph/0012100].
- [4] P. Nath and M. Yamaguchi, Phys. Rev. D **60** (1999) 116006 [arXiv:hep-ph/9903298].
- [5] D. Chakraverty, K. Huitu and A. Kundu, Phys. Lett. B **558** (2003) 173 [arXiv:hep-ph/0212047].
- [6] A.J. Buras, M. Spranger and A. Weiler, Nucl. Phys. B **660** (2003) 225 [arXiv:hep-ph/0212143]; A.J. Buras, A. Poschenrieder, M. Spranger and A. Weiler, Nucl. Phys. B **678** (2004) 455 [arXiv:hep-ph/0306158].
- [7] K. Agashe, N.G. Deshpande and G.H. Wu, Phys. Lett. B **514** (2001) 309 [arXiv:hep-ph/0105084].
- [8] J.F. Oliver, J. Papavassiliou and A. Santamaria, Phys. Rev. D **67** (2003) 056002 [arXiv:hep-ph/0212391].
- [9] T.G. Rizzo and J.D. Wells, Phys. Rev. D **61** (2000) 016007 [arXiv:hep-ph/9906234]; A. Strumia, Phys. Lett. B **466** (1999) 107 [arXiv:hep-ph/9906266]; C.D. Carone, Phys. Rev. D **61** (2000) 015008 [arXiv:hep-ph/9907362].

- [10] T. Rizzo, Phys. Rev. D **64** (2001) 095010 [arXiv:hep-ph/0106336]; C. Macesanu, C.D. McMullen and S. Nandi, Phys. Rev. D **66** (2002) 015009 [arXiv:hep-ph/0201300]; Phys. Lett. B **546** (2002) 253 [arXiv:hep-ph/0207269]; H.-C. Cheng, Int. J. Mod. Phys. A **18** (2003) 2779 [arXiv:hep-ph/0206035]; A. Muck, A. Pilaftsis and R. Rückl, Nucl. Phys. B **687** (2004) 55 [arXiv:hep-ph/0312186].
- [11] H.C. Cheng, K.T. Matchev and M. Schmaltz, Phys. Rev. D **66** (2002) 036005 [arXiv:hep-ph/0204342].
- [12] M. Puchwein and Z. Kunszt, Annals Phys. **311** (2004) 288 [arXiv:hep-th/0309069].
- [13] H. Georgi, A. K. Grant and G. Hailu, Phys. Lett. B **506** (2001) 207 [arXiv:hep-ph/0012379].
- [14] G. von Gersdorff, N. Irges and M. Quiros, Nucl. Phys. B **635** (2002) 127 [arXiv:hep-th/0204223].
- [15] See the website: <http://hep-www.colorado.edu/SUSY>, in particular, N. Danielson, COLO HEP 423. See also, M. Battaglia and D. Schulte, arXiv:hep-ex/0011085; H. Baer, T. Krupovnickas and X. Tata, JHEP **0406** (2004) 061 [arXiv:hep-ph/0405058].
- [16] M.E. Peskin, private communications.
- [17] H.C. Cheng, K.T. Matchev and M. Schmaltz, Phys. Rev. D **66** (2002) 056006 [arXiv:hep-ph/0205314].
- [18] Physics at the CLIC multi-TeV linear collider, Eds: M. Battaglia, A. De Roeck, J. Ellis and D. Schulte, CERN Report No: CERN-2004-005. See also, M. Battaglia, A. Datta, A. De Roeck, K. Kong and K. T. Matchev, arXiv:hep-ph/0502041.
- [19] G. Weiglein *et al.* [LHC/LC Study Group], arXiv:hep-ph/0410364.
- [20] See, for example, Table 5.14 of Ref. [19].
- [21] J. M. Smillie and B. R. Webber, arXiv:hep-ph/0507170.
- [22] B. Bhattacharjee and A. Kundu, arXiv:hep-ph/0508170.
- [23] J. Kalinowski, arXiv:hep-ph/0410137.

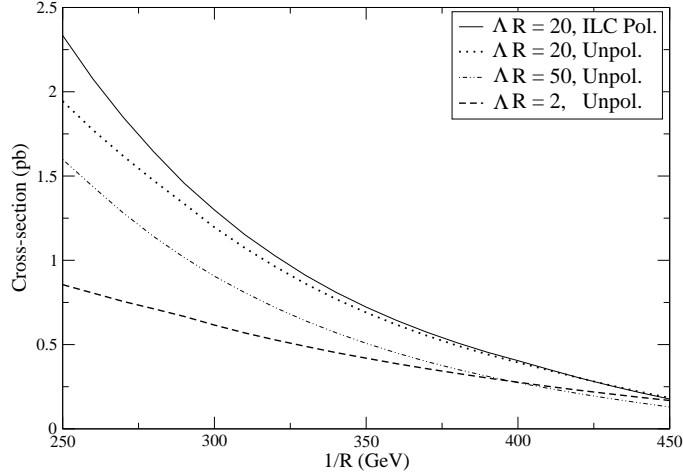


Figure 1: Cross section versus $1/R$ for the process $e^+e^- \rightarrow e^+e^- + \text{missing energy}$. Plots are shown for unpolarised incident beams with $\Lambda R = 2, 20$ and 50 , and for ‘optimum’ ILC polarisation (80% for e^- and 50% for e^+ beams) for $\Lambda R = 20$. The lower and upper energy cuts on the final state leptons are set at 0.5 and 20 GeV, respectively. The angular cuts with respect to the beam axis are set at 15° .

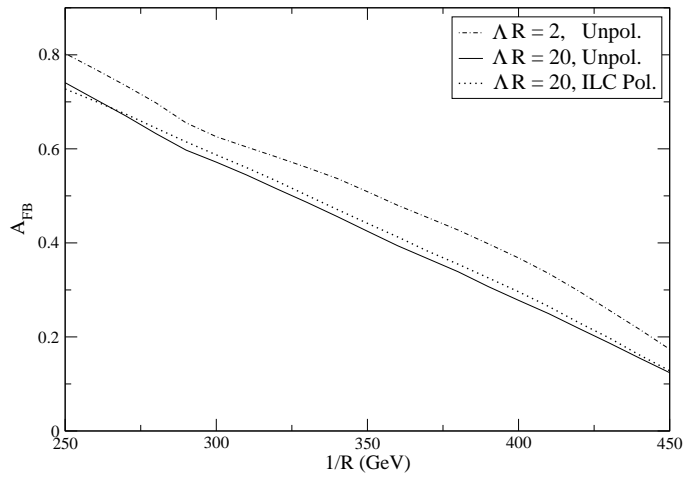


Figure 2: A_{FB} versus $1/R$ for the same process. Plots are shown for unpolarised incident beams with $\Lambda R = 2$ and 20 , and for ‘optimised’ ILC polarisation for $\Lambda R = 20$. The cuts are as in Fig. 1.